

Finite Control Set Model Predictive Control with an Output Current Observer in the dq -Synchronous Reference Frame for an Uninterruptible Power Supply System

Eduardo Zafra
Universidad de Sevilla
Seville, Spain,
ezafra1@us.es

Sergio Vazquez
Universidad de Sevilla
Seville, Spain,
sergi@us.es

Tobias Geyer
ABB Corporate Research
5405 Baden-Dättwil, Switzerland
t.geyer@ieee.org

Francisco J. González
Universidad de Sevilla
Seville, Spain,
fragonrod8@gmail.com

Abraham Marquez
Universidad de Sevilla
Seville, Spain,
amarquez@zipi.us.es

Jose I. Leon
Universidad de Sevilla
Seville, Spain,
jileon@us.es

Leopoldo G. Franquelo^{1,2}
¹Universidad de Sevilla,²Harbin Institute of Technology,
¹Seville, Spain, ²Harbin, China,
¹lgfranquelo@us.es, ²lgfranquelo@hit.edu.cn

Abstract—This work focuses on a Finite Control Set Model Predictive Control (FCS-MPC) method for controlling the output voltage of a two-level three-phase power converter with an output LC filter. This type of control has been proven to be a suitable strategy for uninterruptible power supply (UPS) systems, capable of achieving a high quality output voltage with fast dynamic response. In contrast to previously proposed FCS-MPC strategies, the control problem will be formulated and solved in the synchronous dq -frame. Parameters like the output voltage total harmonic distortion (THD) and the root mean square (RMS) error when tracking the reference voltage will be the focus of the analysis when comparing the output quality.

I. INTRODUCTION

Two-level Voltage Source Inverter (VSI) based applications require high levels of harmonic quality for the voltages, as for example Uninterruptible Power Supplies (UPS) [1]. UPS systems have been extensively studied in academic works and applied in industry for a continuous, reliable supply of critical loads, such as medical equipment, telecommunication systems and computers [2].

Several techniques have been proposed and utilized to eliminate or reduce harmonic content in the output voltage. For example, resonant or repetitive control have been proposed to suppress certain harmonics [3], [4]. Other solutions rely on output LC filters. For this configuration, predictive control, and Finite Control Set Model Predictive Control (FCS-MPC) in particular, are a fertile field in research due to their fast dynamic response and inherent flexibility to consider different control targets, system constraints and nonlinearities [5]–[7].

The application of FCS-MPC for UPS requires an accurate model of the VSI and the output filter in order to predict the evolution of certain system variables up to predetermined horizon length. This model has been previously developed using the stationary $\alpha\beta$ frame [8], [9]. In these works, a FCS-MPC strategy was developed with the addition of an

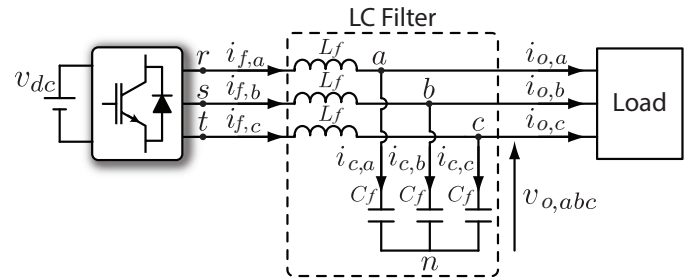


Fig. 1. Three-phase inverter with output LC filter diagram

output current observer that allows the enhancement of the proposed control without increasing the cost of the system with additional sensors. The feasibility of this control strategy was demonstrated through simulation and experimental results.

In this paper, FCS-MPC for UPS application is proposed in a synchronous dq reference frame (dq -SRF). An Extended State Observer (ESO) is also used to estimate the output currents of the system. We will compare the control performance of this FCS-MPC strategy when working in a synchronous dq -frame against a stationary $\alpha\beta$ frame.

Derivation of the system model in dq -frame and the observer are presented in Sections II and III, respectively. In Section IV, the MPC algorithm is formulated. Section V focuses on the pole placement problem to accomplish the tuning of the design parameters. Simulation results are presented and analyzed in Section VI. Computational costs comparison is performed in Section VII.

II. SYSTEM MODEL

In a FCS-MPC strategy, the controller needs to make predictions of future state variables so that a cost function can be evaluated. Depending on this cost function, the next

TABLE I
SYSTEM VARIABLES AND PARAMETERS

Variable	Description
$v_{i,dq}$	VSI output voltage in dq -SRF
$v_{o,dq}$	Output filter capacitor voltage in dq -SRF
$i_{f,dq}$	Output filter inductor current in dq -SRF
$i_{o,dq}$	Output load current in dq -SRF
L_f	Output filter inductor
C_f	Output filter capacitance
v_{dc}	DC-link voltage
ω	Angular frequency of the output reference voltage

switching state is chosen. The predictions of the system are based on a mathematical model that describes the behavior of the electric circuit of the inverter and the LC filter, which is represented in Fig. 1. We will Model the inverter as a system with a finite number of states. The system variables for the inverter can be found in Table I.

Based on the equations in [8], the system dynamic equations in the synchronous dq -frame can be derived:

$$L_f \frac{di_{f,dq}}{dt} = -J\omega L_f i_{f,dq} + v_{i,dq} - v_{o,dq} \quad (1)$$

$$C_f \frac{dv_{o,dq}}{dt} = -J\omega C_f v_{o,dq} + i_{i,dq} - i_{o,dq} \quad (2)$$

where $J = \begin{bmatrix} 0 & -1 \\ 1 & 0 \end{bmatrix}$, and $v_{i,dq}, v_{o,dq}, i_{f,dq}, i_{o,dq} \in \mathbb{R}^2$.

Additionally, $v_{i,dq} = v_{dc} S_{dq}$, where $S_{dq} \in \mathbb{R}^2$ is the switching state of the inverter, expressed in the synchronous dq -frame.

In state-space representation, this model can be summarized with the dynamical equation:

$$\frac{dx}{dt} = Ax + Bu \quad (3)$$

$$y = x \quad (4)$$

where:

$$x = y = \begin{bmatrix} i_{f,dq} \\ v_{o,dq} \end{bmatrix}, u = \begin{bmatrix} v_{i,dq} \\ i_{o,dq} \end{bmatrix}, A = \begin{bmatrix} -J\omega & -\frac{1}{L_f}I_2 \\ \frac{1}{C_f}I_2 & -J\omega \end{bmatrix},$$

$$B = \begin{bmatrix} \frac{1}{L_f}I_2 & O_2 \\ O_2 & -\frac{1}{C_f}I_2 \end{bmatrix}$$

with being I_2 the identity matrix and O_2 a null matrix, both are of 2×2 dimension.

III. EXTENDED-STATE OBSERVER

As seen in Section II, the output currents are part of the input of the system in its state-space representation, so their values are needed. Instead of using their measured values, which would require the addition of sensors, an Extended State Observer (ESO) will be used to obtain estimated values of the output currents. Considering linear output loads that consume sinusoidal currents, and working in a dq -SRF, the output currents can be assumed constant in steady-state. This

is one of the main differences that arise when using the dq -SRF representation of the system model, since system variables in the stationary $\alpha\beta$ frame are sinusoidal waveforms.

Also, due to this fact, the dynamic behavior of the output currents can be expressed by the differential equation:

$$\frac{di_o}{dt} = 0 \quad (5)$$

In contrast to [8], this equation is not just an approximation, since system variables are constant quantities in a dq -SRF. In relation to this fact, a sinusoidal output load model was considered in [9] for the $\alpha\beta$ frame. Due to these differences, the performance of the observer and the control scheme will be analyzed to check how the output voltage quality is affected by these changes.

Considering (5) for the output currents, the system state can be extended to: $x_{dq} = [i_{f,dq}^T \ v_{o,dq}^T \ i_{o,dq}^T]^T$. The extended system in the dq -SRF is then given by:

$$\frac{dx_{dq}}{dt} = \begin{bmatrix} -J\omega & -\frac{1}{L_f}I_2 & O_2 \\ \frac{1}{C_f}I_2 & -J\omega & -\frac{1}{C_f}I_2 \\ O_2 & O_2 & O_2 \end{bmatrix} x_{dq} + \begin{bmatrix} \frac{1}{L_f}I_2 \\ O_2 \\ O_2 \end{bmatrix} v_{i,dq} \quad (6)$$

The output currents are now included in the state vector, so the output of the system is:

$$y_{dq} = \begin{bmatrix} i_{f,dq} \\ v_{o,dq} \end{bmatrix} = C_{dq} x_{dq} \quad (7)$$

with the matrix:

$$C_{dq} = \begin{bmatrix} I_2 & O_2 & O_2 \\ O_2 & I_2 & O_2 \end{bmatrix} \quad (8)$$

Adding a correcting term based on the measured output to the extended model, an observer can be used to estimate the state vector x_{dq} . The estimated state vector is the variable $\hat{x}_{dq} = [\hat{i}_{f,dq}^T \ \hat{v}_{o,dq}^T \ \hat{i}_{o,dq}^T]^T$. Consequently, the observer system is:

$$\frac{d\hat{x}_{dq}}{dt} = A_{e,dq} \hat{x}_{dq} + B_{e,dq} v_{i,dq} + G_{dq} (y_{dq} - C_{dq} \hat{x}_{dq}) \quad (9)$$

where:

$$A_{e,dq} = \begin{bmatrix} -J\omega & -\frac{1}{L_f}I_2 & O_2 \\ \frac{1}{C_f}I_2 & -J\omega & -\frac{1}{C_f}I_2 \\ O_2 & O_2 & O_2 \end{bmatrix}, B_{e,dq} = \begin{bmatrix} \frac{1}{L_f}I_2 \\ O_2 \\ O_2 \end{bmatrix}.$$

In this equation, $G_{dq} \in \mathbb{R}^{6 \times 4}$ is the observer gain matrix, which defines the performance of the observer.

The measured values $i_{f,dq}$ and $v_{o,dq}$ can be considered together with $v_{i,dq}$ as an input, resulting in:

$$\frac{d\hat{x}_{dq}}{dt} = [A_{e,dq} - G_{dq} C_{dq}] \hat{x}_{dq} + [B_{e,dq} \ G_{dq}] \begin{bmatrix} v_{i,dq} \\ i_{f,dq} \\ v_{o,dq} \end{bmatrix} \quad (10)$$

or

$$\frac{d\hat{x}_{dq}}{dt} = A_{obs,dq} \hat{x}_{dq} + B_{obs,dq} u_{obs,dq} \quad (11)$$

where: $A_{obs,dq} = [A_{e,dq} - G_{dq}C_{dq}]$ and $B_{obs,dq} = [B_{e,dq} G_{dq}]$.

The gain matrix G_{dq} will have an important influence on the performance of the FCS-MPC controller. Generally, lower values for this matrix will cause a less noisy output, but a slower dynamic response, so a trade-off must be achieved when tuning these parameters. The values of this matrix are chosen using pole placement of the observer system such that a fast dynamic response is achieved while keeping the noise limited.

IV. CONTROL ALGORITHM

Using the models as basis, and in a similar way to [8], the control algorithm first calculates the estimates of the output currents in the dq -SRF based on the previous values of the estimated and measured variables. Then, a prediction for the next sampling interval ($k + 1$) is calculated from the current switching state, the measured variables and the estimated currents. This prediction is made to compensate the digital delay [10], [11]. In order to choose the next switching state, a cost function that calculates the squared error between the output voltage and the voltage reference in the sampling interval ($k + 2$) is minimized. This cost function is:

$$g = \|v_{o,dq}^*(k+2) - v_{o,dq}(k+2)\|_2^2 \quad (12)$$

To achieve this, all the possible voltages corresponding to the different switching states are calculated using an Exhaustive Searching Algorithm (ESA). For the two-level converter, 7 different states must be evaluated. The state that minimized the cost function will be applied in the next interval of the control algorithm ($k + 1$).

It must be noted that in order to perform this algorithm the continuous-time models introduced in Sections II and III must be discretized for the sampling interval T_s .

V. POLE PLACEMENT

One of the main characteristics of the proposed FCS-MPC is the absence of tuning parameters that modify the behavior of the controller. The selection of the cost function determines the behavior of the control algorithm and which state will be chosen as the optimal one depending on the values of the system variables. In this case, an observer for the output currents was considered, whose dynamics are defined by the matrix gain G_{dq} . As the estimated output currents are one of the inputs to the system, changing the behavior of the observer will affect the general performance of the controller and the quality of the resulting output voltages. Therefore, the gain matrix of the observer becomes the main design parameter for the system. Basically, choosing this gain matrix becomes a pole placement problem where G_{dq} can be calculated through placing the poles of the matrix $A_{obs} = [A_{e,dq} - G_{dq}C_{dq}]$ in order to achieve the preferred performance. In [8], the poles of the observer are simply chosen in a way that ensures a faster dynamic response than the open-loop system (no observer), which can be achieved by looking at the pole-zero map with both the poles of the original system and the poles of the

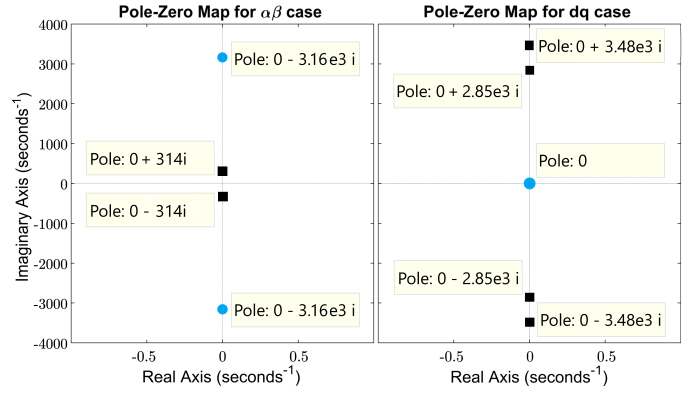


Fig. 2. Pole-Zero map for both systems. Black squares indicate only one pole is in that position. Blue circles indicate that two poles are placed in that spot. Total number of poles for both systems must be 6 (dimension of the system).

observer and ensuring that the observer poles are shifted by a certain amount to the left in the real axis (in the continuous-time system). A similar strategy is followed in [9].

Hereafter, we compare the $\alpha\beta$ formulation with the dq case. Note that their poles are not placed in the same position in the s -plane, as can be seen in Fig. 2.

First, the expression of the system in the $\alpha\beta$ frame is obtained from [9]. It can be noticed that this is the system where the dynamic of the load is approximated by a sinusoidal behavior, which was proven to be a more robust model than the constant model in [8], allowing one to tune the gain matrix for a wider range of load values:

$$\frac{dx_{\alpha\beta}}{dt} = \begin{bmatrix} O_2 & -\frac{1}{L_f}I_2 & O_2 \\ \frac{1}{C_f}I_2 & O_2 & -\frac{1}{C_f}I_2 \\ O_2 & O_2 & J\omega \end{bmatrix} x_{\alpha\beta} + \begin{bmatrix} \frac{1}{L_f}I_2 \\ O_2 \\ O_2 \end{bmatrix} v_{i,\alpha\beta} \quad (13)$$

$$y_{\alpha\beta} = C_{\alpha\beta}x_{\alpha\beta} \quad (14)$$

Similarly to the dq case, the observer system is:

$$\frac{d\hat{x}_{\alpha\beta}}{dt} = \underbrace{[A_{e,\alpha\beta} - G_{\alpha\beta}C_{\alpha\beta}]}_{A_{obs,\alpha\beta}} \hat{x}_{\alpha\beta} + \underbrace{[B_{e,\alpha\beta} G_{\alpha\beta}]}_{B_{obs,\alpha\beta}} \underbrace{\begin{bmatrix} v_{i,\alpha\beta} \\ i_{f,\alpha\beta} \\ v_{o,\alpha\beta} \end{bmatrix}}_{u_{obs,\alpha\beta}} \quad (15)$$

We transform the system in (15) to the dq -SRF by means of the rotation matrix $R = \begin{bmatrix} \cos(\theta) & \sin(\theta) \\ -\sin(\theta) & \cos(\theta) \end{bmatrix}$, where θ corresponds to the phase of the output voltage reference. Assuming that ω is constant, θ can be expressed as: $\theta = \omega t + \theta_0$. Then, the system variables in dq can be expressed as:

$$\begin{bmatrix} i_{f,dq} \\ v_{o,dq} \\ i_{o,dq} \end{bmatrix} = \underbrace{\begin{bmatrix} R & O_2 & O_2 \\ O_2 & R & O_2 \\ O_2 & O_2 & R \end{bmatrix}}_{R_3} \begin{bmatrix} i_{f,\alpha\beta} \\ v_{o,\alpha\beta} \\ i_{o,\alpha\beta} \end{bmatrix} \quad (16)$$

This allows us to write

$$\hat{x}_{dq} = R_3 \hat{x}_{\alpha\beta}, \quad (17)$$

$$\hat{x}_{\alpha\beta} = R_3^{-1} \hat{x}_{dq}, \quad (18)$$

$$u_{obs,\alpha\beta} = R_3^{-1} u_{obs,dq}, \quad (19)$$

$$\text{where } R_3^{-1} = \begin{bmatrix} R^{-1} & O_2 & O_2 \\ O_2 & R^{-1} & O_2 \\ O_2 & O_2 & R^{-1} \end{bmatrix}.$$

Applying (18) and (19) to (15) and left-multiplying it by R_3 , leads to the following expression:

$$R_3 \frac{d(R_3^{-1} \hat{x}_{dq})}{dt} = R_3 A_{obs,\alpha\beta} R_3^{-1} \hat{x}_{dq} + R_3 B_{obs,\alpha\beta} R_3^{-1} u_{obs,dq} \quad (20)$$

Applying the chain rule, the left side of (20) can be rewritten as:

$$\underbrace{\omega \begin{bmatrix} J & O_2 & O_2 \\ O_2 & J & O_2 \\ O_2 & O_2 & J \end{bmatrix}}_{J_3} \hat{x}_{dq} + \frac{d\hat{x}_{dq}}{dt} = \omega J_3 \hat{x}_{dq} + \frac{d\hat{x}_{dq}}{dt} = R_3 A_{obs,\alpha\beta} R_3^{-1} \hat{x}_{dq} + R_3 B_{obs,\alpha\beta} R_3^{-1} u_{obs,dq} \quad (21)$$

In order to simplify the right side of the equation, the following result must be considered:

$$R \begin{bmatrix} a & b \\ -b & a \end{bmatrix} R^{-1} = \begin{bmatrix} a & b \\ -b & a \end{bmatrix} \quad (22)$$

Note that $A_{e,\alpha\beta}$, $B_{e,\alpha\beta}$ and $C_{\alpha\beta}$ consist of submatrices of the type as in (22). To use (22), the gain matrix $G_{\alpha\beta}$ should have the following structure:

$$G_{\alpha\beta} = \begin{bmatrix} G_1 & G_2 \\ G_3 & G_4 \\ G_5 & G_6 \end{bmatrix} = \begin{bmatrix} ag_1 & bg_1 & ag_2 & bg_2 \\ -bg_1 & ag_1 & -bg_2 & ag_2 \\ ag_3 & bg_3 & ag_4 & bg_4 \\ -bg_3 & ag_3 & -bg_4 & ag_4 \\ ag_5 & bg_5 & ag_6 & bg_6 \\ -bg_5 & ag_5 & -bg_6 & ag_6 \end{bmatrix}. \quad (23)$$

If $G_{\alpha\beta}$ has indeed the structure in (23), (21) can be applied, resulting in:

$$\omega J_3 \hat{x}_{dq} + \frac{d\hat{x}_{dq}}{dt} = A_{obs,\alpha\beta} \hat{x}_{dq} + B_{obs,\alpha\beta} u_{obs,dq}, \quad (24)$$

which is equivalent to:

$$\frac{d\hat{x}_{dq}}{dt} = [A_{obs,\alpha\beta} - \omega J_3] \hat{x}_{dq} + B_{obs,\alpha\beta} u_{obs,dq}. \quad (25)$$

To ensure that both closed-loop systems achieve the same behavior, we equate (25) with the dq -SRF observer system in (10). This leads to:

$$A_{obs,\alpha\beta} - \omega J_3 = A_{obs,dq}, \quad (26)$$

$$B_{obs,\alpha\beta} = B_{obs,dq}. \quad (27)$$

Equation (26) can be rewritten as:

$$A_{e,\alpha\beta} - G_{\alpha\beta} C_{\alpha\beta} - \omega J_3 = A_{e,dq} - G_{dq} C_{dq} \quad (28)$$

Taking into account that $C_{\alpha\beta}$ and C_{dq} are the same matrix, and the fact that as it can be noticed from (9) and (13), $A_{e,\alpha\beta} - \omega J_3 = A_{e,dq}$, we obtain the condition:

$$G_{\alpha\beta} = G_{dq} \quad (29)$$

The same condition can be obtained from (27). Consequently, if the gain matrix is tuned to have the structure proposed in (23), it can be established that the gain matrices for both systems will be the same, and indeed both observer systems will have identical expressions. What is willing is pole placement strategy to achieve a gain matrix with the structure in (23).

Searching for different methods and strategies in order to accomplish this, it was found that a dead-beat strategy [12] provides a gain matrix with such a structure. A dead-beat response ensures the stabilization of the observer's estimates in a number of sampling intervals equal to the dimension of the system. A response of this type can be achieved if the poles of the observer's discrete-time system matrix A_{obs} are placed in the origin of the Z-plane. Dead-beat response is usually regarded as too aggressive in the literature. Indeed, a noisy estimate of the currents is expected with these parameters. Tuning strategies with better noise rejection can be found individually for each controller, but differences in the reference tracking of the output voltage are small. This is due to inherent inaccuracies in the prediction model that doesn't consider parasitic elements in the circuit or power losses in the semiconductors. Thus, noisier estimates of the currents will not directly translate into a worse control performance up to a certain level of noise. Plus, this strategy is well suited to comparing both controllers by fulfilling the requirement in (23).

Knowing the location for the poles of the observer system, the calculation of the gain matrix G_{dq} is reduced to a pole placement problem that can be solved with different methods.

VI. SIMULATION RESULTS

In this section, the performance for both controllers will be assessed through simulations with Matlab-Simulink. Parameters for the system can be found in Table II.

Output voltage regulation is shown in the abc -frame in Fig. 3. To check the transient response, the load is connected at 130 milliseconds in simulation time, so the effect in voltage regulation can be seen. It can be noticed that the output voltage is regulated to its given reference. Also, real output currents are compared with the observed currents estimated by the observer in Fig. 4. As expected, the output of the observer presents noticeable noise because of the dead-beat tuning. The RMS error in the output voltage tracking, and the current estimation is compared in Fig. 5 for both cases. Finally, the harmonic

TABLE II
PARAMETERS FOR SIMULATIONS

Parameters	Value
DC-Link Voltage [V]	700
Reference Phase Voltage Amplitude [Vph-n]	200
Filter Capacitor [μ F]	50
Filter Inductor [mH]	2
Load Resistance [Ω]	15
Load Inductor [mH]	20
Sampling Interval [μ s]	40

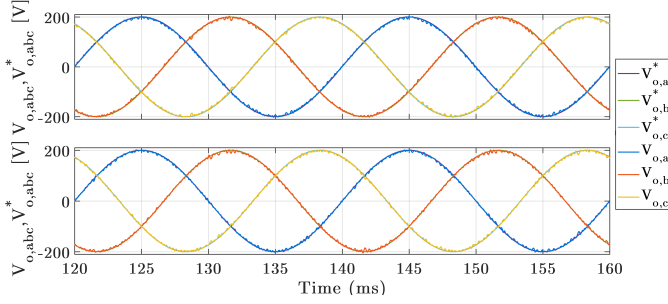


Fig. 3. Output voltages with their references in abc -frame. Top: dq . Bottom: $\alpha\beta$.

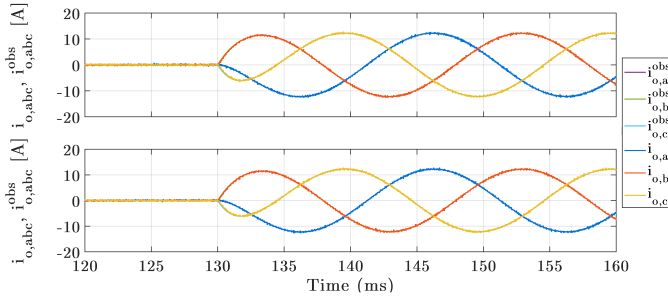


Fig. 4. Real and observed output currents in abc -frame. Top: dq . Bottom: $\alpha\beta$.

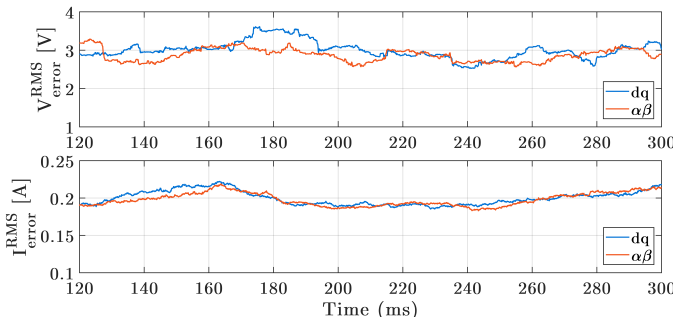


Fig. 5. RMS error for voltage reference tracking (top) and current estimation (bottom) for variables corresponding to phase a .

spectra of the output voltages are shown in Fig. 6. While the tracking error for the output voltages stays at around the same level, a small reduction in the THD is achieved in the dq -case.

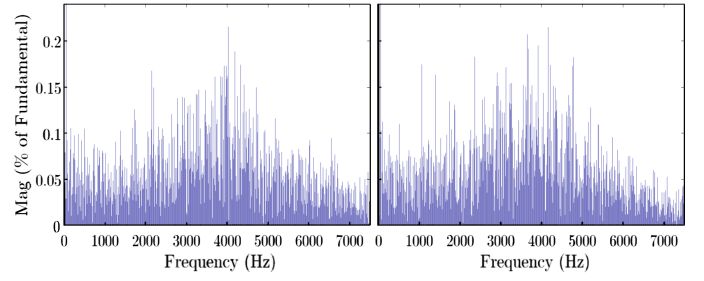


Fig. 6. Harmonic analysis of the output voltage up to 7500 Hz. THD = 1.61 % for dq (left graph) and THD = 1.70 % for $\alpha\beta$ (right graph).

TABLE III
NUMBER OF OPERATIONS

Parameters	Sums	Multiplications
dq	290	330
$\alpha\beta$	183	232

VII. COMPUTATIONAL COSTS

Besides the control performance of both methods, the computational burden may also be an important characteristic that can affect the decision of using one reference frame or the other. As far as the computational costs of the algorithm are concerned, more operations have to be made when computing the algorithm in the dq -frame. This is due to the extra transformation of the model variables to the dq -frame. The number of operations for both strategies is summarized in Table III

Regarding memory resources, dq formulation presents the advantage of being able to work with a constant reference, while in $\alpha\beta$ a sinusoidal reference must be generated or tabulated. On the other hand, sine and cosine values have to be calculated or tabulated in dq in order to transform variables, so memory consumption is similar in both cases.

VIII. CONCLUSION

In this paper, a revised FCS-MPC controller for UPS applications, which was originally proposed in [8], [9] in a stationary $\alpha\beta$ frame, was designed in the dq -synchronous reference frame. Models for the three-phase two-level VSI with output LC filter and the output current observer were derived in dq -SRF in order to obtain the system equations needed for the controller.

An analysis of the pole placement of the observer was accomplished, in order to obtain values of the gain matrices that allow a fair comparison of the controllers in both reference systems. In particular, a dead-beat tuning for the observer was found to be a good option in order to carry out this comparison.

Comparative results between $\alpha\beta$ with sinusoidal output load model and dq controllers were obtained by simulation. Output current estimation and voltage tracking performed in dq -SRF achieve a fast dynamic response when a load is connected to the system, with very similar performance to the $\alpha\beta$ case, when the load is approximated with a sinusoidal behavior.

Reference tracking error and estimation error evolve at around the same level for both cases. THD presents a small reduction in the dq -case, decreasing from 1.70 % in $\alpha\beta$ to 1.61 % in dq .

Last, the computational cost was compared, by showing the number of operations in each case. The case $\alpha\beta$ proved to have a smaller computational burden because of the absence of the Park transformation.

REFERENCES

- [1] F.-S. Pai and S.-J. Huang, "A novel design of line-interactive uninterruptible power supplies without load current sensors," *IEEE Transactions on Power Electronics*, vol. 21, DOI 10.1109/TPEL.2005.861188, no. 1, pp. 202–210, Jan. 2006.
- [2] J. M. Guerrero, L. Garcia De Vicuna, and J. Uceda, "Uninterruptible power supply systems provide protection," *IEEE Industrial Electronics Magazine*, vol. 1, DOI 10.1109/MIE.2007.357184, no. 1, pp. 28–38, Spring 2007.
- [3] S. Chen, Y. M. Lai, and C. K. Tse, "Optimal design of repetitive controller for harmonic elimination in pwm voltage source inverters," in *INTELEC 07 - 29th International Telecommunications Energy Conference*, DOI 10.1109/INTLEC.2007.4448774, pp. 236–241, Sep. 2007.
- [4] M. Castilla, J. Miret, A. Camacho, J. Matas, and L. G. de Vicuna, "Reduction of current harmonic distortion in three-phase grid-connected photovoltaic inverters via resonant current control," *IEEE Transactions on Industrial Electronics*, vol. 60, DOI 10.1109/TIE.2011.2167734, no. 4, pp. 1464–1472, Apr. 2013.
- [5] S. Vazquez, J. Rodriguez, M. Rivera, L. G. Franquelo, and M. Norambuena, "Model predictive control for power converters and drives: Advances and trends," *IEEE Transactions on Industrial Electronics*, vol. 64, DOI 10.1109/TIE.2016.2625238, no. 2, pp. 935–947, Feb. 2017.
- [6] S. Vazquez, J. I. Leon, L. G. Franquelo, J. Rodriguez, H. A. Young, A. Marquez, and P. Zanchetta, "Model predictive control: A review of its applications in power electronics," *IEEE Industrial Electronics Magazine*, vol. 8, DOI 10.1109/MIE.2013.2290138, no. 1, pp. 16–31, Mar. 2014.
- [7] P. Cortes, M. P. Kazmierkowski, R. M. Kennel, D. E. Quevedo, and J. Rodriguez, "Predictive control in power electronics and drives," *IEEE Transactions on Industrial Electronics*, vol. 55, DOI 10.1109/TIE.2008.2007480, no. 12, pp. 4312–4324, Dec. 2008.
- [8] P. Cortes, G. Ortiz, J. I. Yuz, J. Rodriguez, S. Vazquez, and L. G. Franquelo, "Model predictive control of an inverter with output LC filter for ups applications," *IEEE Transactions on Industrial Electronics*, vol. 56, DOI 10.1109/TIE.2009.2015750, no. 6, pp. 1875–1883, Jun. 2009.
- [9] S. Vazquez, A. Marquez, J. I. Leon, L. G. Franquelo, and T. Geyer, "FCS-MPC and observer design for a VSI with output LC filter and sinusoidal output currents," in *2017 11th IEEE International Conference on Compatibility, Power Electronics and Power Engineering (CPE-POWERENG)*, DOI 10.1109/CPE.2017.7915254, pp. 677–682, Apr. 2017.
- [10] L. Malesani, P. Mattavelli, and S. Buso, "Robust dead-beat current control for PWM rectifiers and active filters," in *Conference Record of 1998 IEEE Industry Applications Conference. Thirty-Third IAS Annual Meeting (Cat. No.98CH36242)*, vol. 2, DOI 10.1109/IAS.1998.730323, pp. 1377–1384 vol.2, Oct. 1998.
- [11] P. Cortes, J. Rodriguez, C. Silva, and A. Flores, "Delay compensation in model predictive current control of a three-phase inverter," *IEEE Transactions on Industrial Electronics*, vol. 59, DOI 10.1109/TIE.2011.2157284, no. 2, pp. 1323–1325, Feb. 2012.
- [12] S. E. Tuna, "Deadbeat observer: Construction via sets," in *Proceedings of the 2011 American Control Conference*, DOI 10.1109/ACC.2011.5990622, pp. 2596–2601, Jun. 2011.